BMC Plant Biology

RESEARCH

Open Access

Metabolome and transcriptome profiling reveals light-induced anthocyanin biosynthesis and anthocyanin-related key transcription factors in Yam (*Dioscorea Alata* L.)

Peipei Zhang[1,2,3,4], Shiqiang Xu[1,4], Long Zhang[1,4], Xulong Li[1,4], Jie Qi[3], Lin Weng[2], Shike Cai[1,4] and Jihua Wang[1,4*]

Abstract

Background Yam is a globally significant crop with both culinary and medicinal value. Anthocyanin, an important secondary metabolite, plays a key role in determining the nutritional quality of yams. However, the research on the light-induced anthocyanins accumulation in yams remains limited. In this study, we revealed light-induced anthocyanin biosynthesis and identified transcription factors associated with anthocyanin-related pathways in yam. These findings enhance our understanding of the molecular mechanisms underlying light-mediated anthocyanin regulation in yams.

Results Significant variations in color were observed in the stems, leaves, and tuber roots of the two yam varieties 'Xuwen' and 'Luhe'. Under light conditions, the total anthocyanin content in 'Xuwen' tuber roots was significantly higher than that under dark conditions. The targeted metabolomics analysis of anthocyanins identified that procyanidin and cyanidin glycosides, such as cyanidin-3-O-(sinapoyl)sophoroside, cyanidin-3-O-sophoroside, procyanidin B1, procyanidin B3, and quercetin-3-O-glucoside, were the primary anthocyanin components. These compounds were responsible for the observed differences in anthocyanin content between the two varieties and were significantly influenced by light conditions. The non-targeted metabolomics analysis further revealed that light also induce the biosynthesis of flavonoids. Transcriptome analysis showed significant differences in the expression levels of MYB, ERF, and WRKY transcription factors (TFs) between the two yam varieties, with these expressions being strongly influenced by light conditions. The association analysis of the anthocyanin metabolome, candidate TFs, and structural genes involved in anthocyanin biosynthesis revealed significant correlations. Specifically, MYB (*Dioal.09G044700* and *Dioal.12G068700*) and WRKY (*Dioal.20G040900* and *Dioal.12G062900*) showed strong correlations with procyanidins, anthocyanins, and the structural genes associated with anthocyanin biosynthesis. RT-qPCR confirmed that the expression patterns of these four TFs, strongly induced by light, were consistent with the expression of structural genes involved in anthocyanin biosynthesis.

*Correspondence:
Jihua Wang
wangjihua@gdaas.cn

Full list of author information is available at the end of the article

Conclusions The results of this study provide useful insights into the regulation of light on anthocyanin accumulation in yam, and will be helpful for yam breeding and cultivation practices.

Keywords Yam, Anthocyanin, Metabolome, Transcriptom, Light, Transcription factors

Background

Yam is a nutrient-rich food that provides essential components for human health, including protein, vitamins, starch, trace elements, and other vital nutrients [1]. Renowned for its crisp texture and sweet flavor, yam is a versatile ingredient in numerous culinary foods. The mucilage polysaccharides present in yam play a significant role in modulating the body's immune system and exhibit notable antioxidant, antiviral, and anti-aging properties [2]. Furthermore, saponins found in yam have been shown to help regulate blood sugar levels, reduce blood lipids, lower uric acid, possess anti-inflammatory effects, demonstrate anticancerous activity, and inhibit tumor growth [3]. The root tuber also contains allantoin, a compound that is believed to enhance wound healing and exhibit anti-inflammatory properties [4]. In the research of traditional Chinese medicine, yam is valued for its ability to strengthen the spleen and stomach, aid digestion, and promote longevity [5]. Additionally, in certain pigment-rich varieties, such as purple yams, anthocyanins emerge as key components within the root tubers [6]. Anthocyanins are a class of plant flavonoid compounds responsible not only for imparting vibrant colors to plants but also for playing a crucial role in their stress responses. These compounds offer protection against oxidation, light damage, and pests/diseases [7, 8]. Moreover, anthocyanins have garnered attention for their diverse health benefits, including anti-inflammatory, antioxidant, anti-obesity, immune-regulating, and neuroprotective properties. As a result, they are extensively utilized in health supplements, pharmaceuticals, cosmetics, and food coloring applications [6, 9, 10]. Given the significant nutritional and medicinal value of anthocyanins, it becomes crucial to identify yam varieties with high anthocyanin content and unravel the genetic regulation behind their biosynthesis.

The biosynthesis of anthocyanins is conserved across the plant kingdom and arises from phenylpropanoid and flavonoid metabolic pathways. Phenylalanine acts as a crucial precursor in the phenylpropanoid pathway. The synthesis of anthocyanins comprises three primary steps (Fig. S1): The initial step involves the formation of p-coumaroyl-CoA, catalyzed by enzymes such as phenylalanine ammonia-lyase (PAL), cinnamic acid 4-hydroxylase (C4H), and 4-coumaric acid CoA ligase (4CL). P-coumaroyl-CoA serves as a precursor for the synthesis of lignin, phenolic acids, and various flavonoid compounds, including flavones, isoflavones, flavonols, and anthocyanins. In the second step, p-coumaroyl CoA undergoes transformation via chalcone synthase (CHS) and chalcone isomerase (CHI) to produce naringenin. Subsequently, naringenin is converted by flavanone 3'-hydroxylase (F3H), flavonoid 3',5'-hydroxylase (F3'5'H), and dihydroflavonol 4-reductase (DFR) into leucopelargonidin, leucocyanidin, leucodelphinidin, and other leucoanthocyanidins. The third step involves the conversion of these leucoanthocyanidins into light red anthocyanins via the catalysis of anthocyanidin synthase (ANS/LDOX) [11]. Additionally, the C3, C5, and C7 positions of anthocyanidins undergo further modifications via glycosylation, methylation, and acylation enzymes, such as anthocyanidin 3-O-glucosyltransferase (BZ1) and anthocyanin 3-O-glucoside-6"-O-malonyltransferase (3MaT1). These modifications enhance the chemical stability and color intensity of anthocyanins, producing pigments like brick red pelargonin glycoside, red cyanidin glycoside, and blue-purple delphin glycoside [12].

In addition to structural genes, TFs, predominantly MYB TFs, play a pivotal role in the regulating anthocyanin biosynthesis by directly or indirectly modulating the transcriptional activity of structural genes. To date, three primary mechanisms by which MYB TFs regulate anthocyanin biosynthesis have been elucidated. In the first type, MYB TFs directly bind to the promoters of structural genes involved in the anthocyanin biosynthesis pathway, thereby modulating genes transcription [13]. In the second type, MYB TFs form a complex with bHLH TFs and WD40 repeat proteins.The MYB-bHLH-WD Repeat (MBW) complex, which subsequently binds to the promoter regions of structural genes involved in anthocyanin synthesis, thereby regulating genes transcription [14]. In the third type, MYB TFs indirectly regulate anthocyanin biosynthesis by interfering with MBW complexes formation, thereby controlling the expression levels of structural genes (Fig. S2) [15].

Beyond genetic factors, environmental factors such as light, temperature, biotic stress, and abiotic stress also significantly influence anthocyanin biosynthesis [8, 16]. Research indicates that most anthocyanins are light-induced, with the quality, intensity, and duration of light directly affecting plants anthocyanin content [17]. In response to light signals, plant photoreceptor systems including PHYTOCHROME (PHY), CRYPTOCHROME (CRY), and ultraviolet B receptors modulate the expression levels of genes associated with anthocyanin synthesis through cellular signaling pathways [18, 19]. Upon sensing light signals, photoreceptors such as PHY, CRY, and UV-B receptors activate specific signal transduction

pathways and induce the expression of the HY5 (HYPocotyl 5), a transcription factor characterized by a leucine zipper motif [20]. In pear (*Pyrus pyrifolia*), HY5 binds to the promoter regions of genes such as *MYB75*/*PAP1*, *PyMYB10*, and *PyWD40*. This binding activates their expression, subsequently enhancing the activity of the MBW complex and fully initiating anthocyanin biosynthesis [21]. In *Arabidopsis*, this regulatory process is balanced by negative feedback from negative regulators such as COP1 [22]. However, the specific light-responsive MYB TF contributing to anthocyanin content remain unidentified in yam.

In this study, the phenotypic characteristics of two yam varieties, 'Luhe' and 'Xuwen' under dark/light conditions were analyzed. Targeted metabolomics of anthocyanidins, non-targeted metabolome analysis, transcriptome analysis, and molecular biology methods were employed in this study. The objectives of this research were twofold: (i) to identify the primary anthocyanin components responsible for the observed color differences between yam varieties under light influence, and (ii) to determine the key genes regulating yam anthocyanin biosynthesis that are influenced by light. This investigation revealed the molecular mechanisms underlying how genetic and light factors impact anthocyanin biosynthesis in yam, identifying candidate TFs that regulate anthocyanin biosynthesis in response to light induction. These findings are conducive to the improvement of yam genetics and cultivation.

Results

Anthocyanin content was simultaneously influenced by genetic and light factors

To examine the effects of genetic and light conditions on anthocyanins in yam, two varieties, 'Luhe' and 'Xuwen', were cultivated in a field setting. This allowed for phenotypic observations and analysis of anthocyanin content. Phenotypic observations revealed that 'Xuwen' displayed significantly more intense purple hues in its stems, leaves, and root tubers compared to 'Luhe'. Furthermore, when root tubers of 'Xuwen' was exposed to natural light (referred to as 'Xuwen-L'), it showed a notably deeper purple coloration than those grown in the dark (Fig. 1A-D). The analysis of total anthocyanin content in the root tubers indicated that 'Xuwen-L' had higher levels than both 'Xuwen' and 'Luhe'. Additionally, 'Xuwen' also exhibited greater anthocyanin content compared to 'Luhe' (Fig. 1E). These findings suggested that the accumulation of anthocyanins in yams was influenced by both genetic factors and light conditions.

Cyanidin glycosides and procyanidins were the main substances affected by genetic and light factors

In order to identify the major anthocyanin components influenced by genetic and light factors, a targeted anthocyanidin metabolome profiling was performed in this study. A total of sixty-three metabolites were identified, including two flavonoids (naringenin and quercetin-3-O-glucoside), five procyanidins, peonidin, and fifty-five anthocyanins (Table S1). These fifty-five anthocyanins comprised twenty-three cyanidin glycosides, seven delphinidin glycosides, five malvidin glycosides, five pelargonidin glycosides, nine peonidin glycosides, five petunidin glycosides, and one peonidin-3-O-(feruloyl) glucuronide. Among the sixty-three metabolites, fifty metabolites exhibited significant differences between the 'Luhe' (White, W), 'Xuwen' (Part-red, P), and 'Xuwen-L' (Full-red, F) (Table S2). These fifty metabolites included the flavonoid quercetin-3-O-glucoside, five procyanidins, and forty-four anthocyanin compounds. Among these forty-four metabolites, there were twenty-one cyanidin glycosides, seven delphinidin glycosides, one malvidin-3-O-glucoside, three pelargonidin glycosides, seven peonidin glycosides, three petunidin glycosides, and two additional peonidin-related compounds (peonidin and peonidin-3-O-(feruloyl) glucuronide).

The results of the principal component analysis (PCA) of differential metabolites (DM) revealed that principal component 1 (PC1) accounted for 86.6% of the total variation, while principal component 2 (PC2) accounted for 4.8% (Fig. 2A). This suggested that PC1 effectively captured significant differences in metabolite data, particularly between group F and the other groups, with groups W and P showing lesser distinctions. These findings implied that light substantially influences anthocyanin metabolism in yam. Analysis of metabolite content across the three sample groups demonstrated a significant positive correlation among all samples (Fig. 2B), suggesting that the relative proportions of each anthocyanin within the groups were consistent. Group F contained forty-nine DM compared to group P, with forty-seven metabolites exhibiting significantly increased levels. Conversely, two metabolites, cyanidin-3-O-(6"-O-coumaryl)xyloside and delphinidin-3-O-(6-O-malonyl-beta-D-glucoside), showed decreased levels (Fig. 2C, Table S2). Comparative analysis between groups F and W identified forty-eight DM, all of which exhibited significantly elevated levels in group F. Additionally, twenty-six DM were observed between groups P and W, with significant increases noted in group P as well. Notably, the total anthocyanin content in group F was higher than that in group P, indicating the positive impact of light on anthocyanin levels within group F (Table S2).

To further investigate whether anthocyanins are affected by both genetic and light factors, the shared

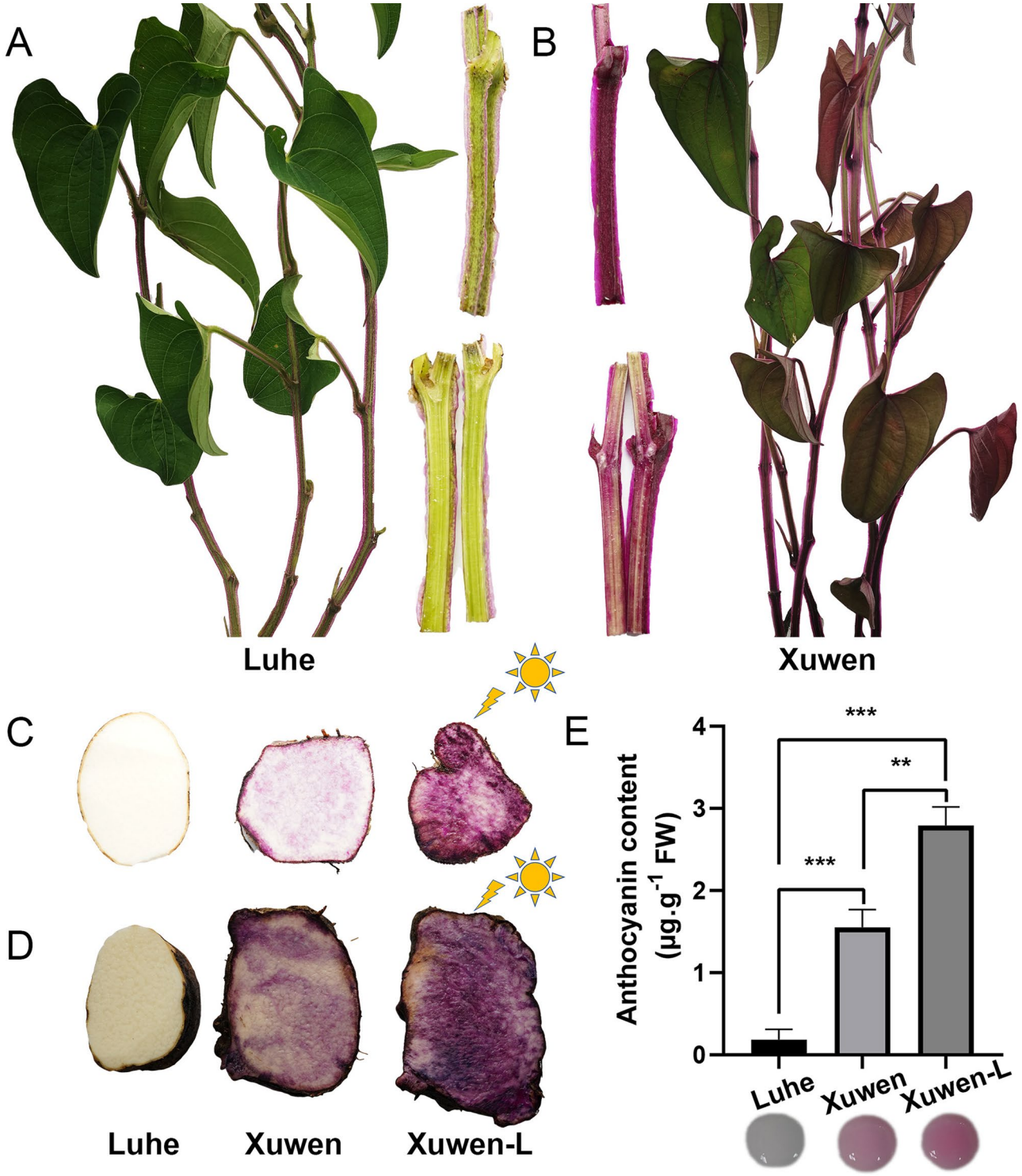

Fig. 1 Phenotype of two yam cultivars. (**A, B**) Stem and leaf phenotype of 'Luhe'/W (**A**) and 'Xuwen'/P (**B**); (**C, D**) Root tubers colors of the two cultivars under different environments conditions and developmental stages. 'Xuwen-L'/F denotes the 'Xuwen' cultivar exposed to light conditions; (**E**) Total anthocyanin content. ** and *** represent significance of $P < 0.01$ and $P < 0.001$, respectively

twenty-three DM from all three comparison groups (group P vs. W, group F vs. W, and group F vs. P) were selected for additional analysis (Fig. 2D, Table S3). These twenty-three DM included twelve cyanidin glycosides, two delphinidin glycosides, three peonidin glycosides, two petunidin glycosides, two proanthocyanidins, as well as quercetin-3-O-glucoside and pelargonidin-3-O-sophoroside. Cluster analysis revealed that the content of

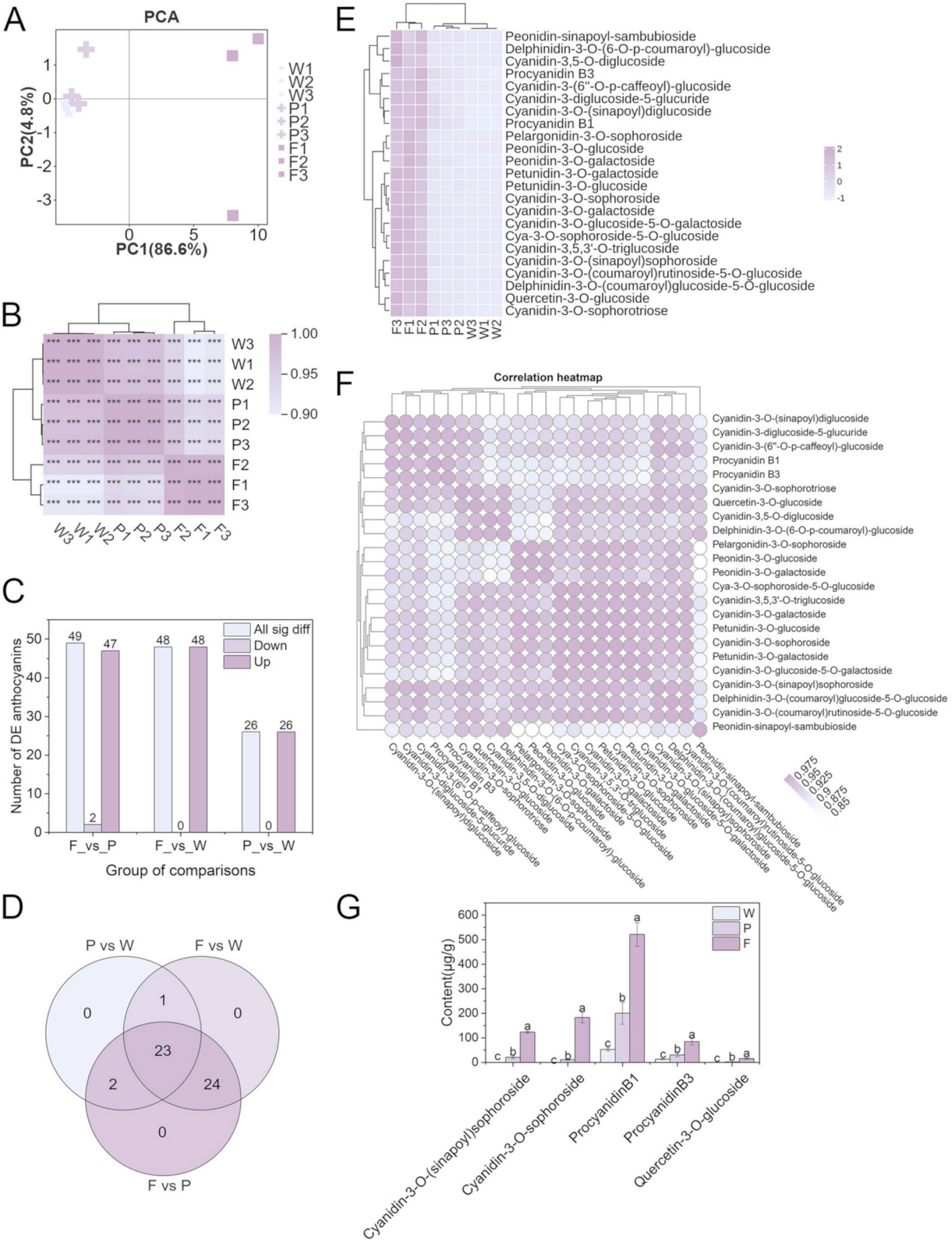

Fig. 2 (See legend on next page.)

(See figure on previous page.)

Fig. 2 Analysis of differential anthocyanin metabolites among W, P and F. (**A**) PCA analysis of DM; (**B**) Pearson correlation analysis of the samples in metabolites content. (**C**) Number of differential anthocyanin metabolites; (**D**) Venn diagram showed the overlap of differential anthocyanin metabolites among the three groups; (**E**) Cluster heat map of twenty-three differential anthocyanin metabolites in the three groups; (**F**) Correlation analysis for the twenty-three differential anthocyanin metabolites in the three groups; (**G**) The five key DM out of the twenty-three anthocyanin metabolites identified in the three groups. Different letters denote significant differences ($P < 0.05$) according to Duncan's multiple range test. The data in figure G is presented as the mean ± SEM. ($n = 3$ biologically independent samples)

these twenty-three DM were higher in group F compared with groups P and W (Fig. 2E). Furthermore, correlation analysis indicated a significant positive correlation among these metabolites (Fig. 2F). Among the twenty-three metabolites in the three groups, five specifically exhibited significant changes in content: cyanidin-3-O-(sinapoyl) sophoroside, cyanidin-3-O-sophoroside, procyanidin B1, procyanidin B3, and quercetin-3-O-glucoside (Fig. 2G). These findings indicated that cyanidin glycosides and proanthocyanidins were the primary compounds influenced by genetic and light factors in the yam anthocyanin metabolic pathway.

The upstream biosynthesis pathway of anthocyanins was influenced by light in Yam

To further elucidate the metabolite differences between the two varieties and their responses to light, a non-targeted metabolomics approach was applied in this study. A total of 15,115 metabolites were detected in the three sets of samples (W, P, and F). PCA analysis of all metabolite content demonstrated good biological replicates within each group (Fig. 3A). Among the 15,115 metabolites, 10,266 exhibited significant concentration differences across sample sets (Table S4). The numbers of upregulated and downregulated DM in each groups are listed in Fig. S3. A total of 3,690 DM were common in the three comparison groups (Fig. S4). Based on molecular weight and MS/MS fragmentation patterns, 199 metabolites were identified (Table S5), predominantly classified as amino acids, lipids, carbohydrates, cofactors, and vitamins (Fig. 3B).

To explore the influence of light on yam biochemical profiles, the 199 previously identified metabolites were further analyzed. The DM were primarily products of the isoquinoline alkaloid, tyrosine, phenylalanine, phenylpropanoid, flavone, and flavonol pathways. Compared to W, P exhibited 101 DM, with 48 metabolites upregulated and 53 downregulated (Table S6). Compared to W, F had 95 DM, with 55 metabolites upregulated and 40 downregulated (Table S7). Compared to P, F had 101 DM, with 60 upregulated and 41 downregulated (Table S8). A total of 68 DM were common in the three comparison groups (Fig. 3C), mainly enriched in phenylpropanoid biosynthesis, flavonoid biosynthesis, flavone and flavonol biosynthesis, betalain biosynthesis, phenylalanine metabolism, purine biosynthesis, sphingolipid metabolism, and zeatin biosynthesis (Fig. 3D). Among the identified 199 metabolites, only one anthocyanin pathway substance, peonidin-3-glucoside, was included. However, 11 flavonoid metabolites out of the 68 DM exhibited a significant correlation with peonidin-3-glucoside (Fig. 3E). This indicates that light may have an impact on the anthocyanin pathway by influencing flavonoid biosynthesis. Cluster analysis revealed that the upstream substances of anthocyanins, including rutin, quercetin, epicatechin, kaempferide, trans-Cinnamate, 2-phenylacetamide, and D-phenyllactic acid, were increased in response to light. Conversely, the concentrations of isosakuranetin, naringenin, N-Acetyl-L-phenylalanine, and naringenin 7-O-beta-D-glucoside were decreased under light conditions (Fig. 3F, Table S9). In conclusion, the upstream biosynthesis pathway of anthocyanins is also influenced by light conditions.

MYB and WRKY may be major candidate genes in yam response to light and regulation of anthocyanins biosynthesis

To explore genes responsive to light and regulating anthocyanin biosynthesis, transcriptome sequencing was performed on three sample groups: W, P, and F. The PCA analysis of all gene expression levels demonstrated high biological replicability among all samples, with P and F groups showing similar gene expression patterns (Fig. 4A). Gene expression levels exhibited positive correlations across samples, with particularly strong correlations noted between the P and F groups (Fig. 4B). Transcriptome sequencing identified 23,363 transcribed genes, of which 7,396 exhibited significant differential expression across all three sample groups. Compared to W, P exhibited 5,385 differentially expressed genes (DEGs), including 3,031 upregulated and 2,354 downregulated genes (Fig. 4C). Similarly, F showed 4,735 DEGs, with 2,609 upregulated genes and 2,126 downregulated. Comparing F to P, there were 2,427 DEGs, with 1,017 upregulated and 1,410 downregulated.

To identify genes that simultaneously respond to light and regulate the biosynthesis of anthocyanins, we used 391 DEGs common to the three comparison groups: P_vs_W, F_vs_W, and F_vs_P for further analysis (Fig. 4D, Table S10). Among these 391 genes, 179 genes showed consistent expression trends in the three comparison groups, of which 159 were upregulated and 20 were downregulated compared to W (Fig. 4E, Table S11). Out of these 179 genes, compared to W, 159 genes

were upregulated, and 20 genes were downregulated, with a total of 165 genes, including 21 TFs, being annotated for their functions (Table S11). Since anthocyanin biosynthesis involves multiple structural genes primarily regulated by TFs, we analyzed these 21 TFs in detail (Table S12). These TFs predominantly belong to the ERF, MYB, WRKY, GATA, HSF, TCP, and bHLH families, with 20 TFs showing upregulation and one TF being downregulated (Fig. 4F). Notably, *Dioal.09G044700* (MYB), *Dioal.04G024500* (ERF), and *Dioal.19G002500* (ERF) showed increased expression levels after light induction.

To further elucidate the TFs that regulate anthocyanin biosynthesis, the aforementioned 21 TFs, along with specific genes involved in anthocyanin biosynthesis (*PAL*, *4CL*, *C4H*, *DFR*, *UGT*), and the competing pathway gene (*I2'H*), were analyzed in correlation with aforementioned 23 differentially expressed metabolites (classified into anthocyanins and procyanidins) that displayed significant differences in the comparison groups (P_vs_W, F_vs_W, F_vs_P) (Fig. 4G). The results demonstrated significant correlations among most TFs, which also showed significant correlations with most structural genes. Notably, two MYB TFs (*Dioal.09G044700* and *Dioal.12G068700*) and two WRKY TFs (*Dioal.20G040900* and *Dioal.12G062900*) exhibited significant correlations with both anthocyanins and procyanidins, suggesting their potential roles as candidate genes in regulating anthocyanin biosynthesis.

The four TFs and most structural genes involved in anthocyanin biosynthesis were induced by light

To further analyze how differences in anthocyanin content induced by light and varieties are primarily regulated by transcription factors, we examined the expression levels of structural genes involved in anthocyanin biosynthesis. The results showed that the expression levels of *PAL*, *C4H*, *4CL*, *CHS*, *DFR*, *BZ1*, and *3MaT1*, which are involved in anthocyanin biosynthesis, were higher in 'Xuwen' compared to 'Luhe'. Additionally, most of these genes exhibited highest expression levels in 'Xuwen-L' (Fig. 5A). The expression patterns of UFGTs and UGTs, which are involved in phenylpropanoid biosynthesis, flavonoid biosynthesis, flavone and flavonol biosynthesis (upstream processes of anthocyanin biosynthesis), were similar to those observed for genes in the anthocyanin synthesis pathway (Fig. 5B). Conversely, the expression pattern of the competing pathway gene *I2'H* was opposite to that of genes in the anthocyanin synthesis pathway (Fig. 5B). We verified the RNA-seq findings using RT-qPCR analysis (Fig. 5C, D). The RT-qPCR results confirmed that light induced the expression levels of TFs and most structural genes involved in anthocyanin biosynthesis, including *PAL2*, *PAL3*, *C4H1*, *C4H2*, *4CL2*, *DFR*, 3*MaT1*, 3*MaT2*, *UFGT2*, *UGT2*, *UGT4*, and *UGT7*. These results suggested that variations in anthocyanin content may arise from the regulation of expression levels of multiple structural genes by TFs, rather than the upregulation of a single structural gene.

Discussion

Currently, few studies have been conducted on the anthocyanins of purple yam. The development of functional health foods using purple yam anthocyanins as nutritional components has significant market potential and can yield positive social and economic outcomes. Purple yam anthocyanins exhibit diverse biological activities and hold significant potential for use as medicinal and nutritional ingredients in various industries, including pharmaceuticals and food. In this study, we identified differences in anthocyanin and other metabolite levels between two varieties of white and purple yams, and examined the impact of light on these compounds. Key transcription factors that regulate anthocyanin content and respond to light were elucidated. This findings provide a theoretical basis for improving yam genetics and cultivation practices to enhance anthocyanin levels, offering valuable insights for agricultural advancements.

Anthocyanins exhibit diverse biological properties, such as anti-mutagenic and anti-cancer effects, anti-hyperglycemic activity, cardiovascular disease prevention, antioxidant properties, and free radical scavenging activities [23, 24]. The purple color in yams is primarily due to the glycosylation, methylation, and acylation of anthocyanidins, which results in darker anthocyanins like brick red pelargonin glycoside, red cyanidin glycoside, and blue-purple delphin glycoside [6]. In this study, we identified twenty-three anthocyanins influenced by both genetic and light factors, with cyanidin glycosides being the predominant anthocyanins. The purple color of yams may primarily result from the cyanidin glycosides. In a previous study, it was found that purple yam contain a variety of acylated anthocyanins [6]. Several studies have also reported the effects of light on anthocyanins in various plants [17, 25]. The specific types of light-induced anthocyanins differ among plant species. For instance, in rabbiteye blueberry, *Capsicum annuum*, and *Lycium ruthenicum*, increased light intensity enhances the accumulation of delphinidin glycoside [26, 27]. Similary, in sweet cherry and apple peel, cyanidin glycoside is significantly influenced by light [28, 29]. These findings suggest that plant coloration patterns are intricately linked to the types of anthocyanins induced by light conditions.

Light signals can induce various signal transduction factors, such as HY5, the COP1/SPA complex, WRKY, and B-box protein. These factors mediate the regulation of light-dependent anthocyanin biosynthesis through MYB TFs and the MBW complex [30]. In *Arabidopsis*, COP1 controls the protein stability of the MYB TFs, such

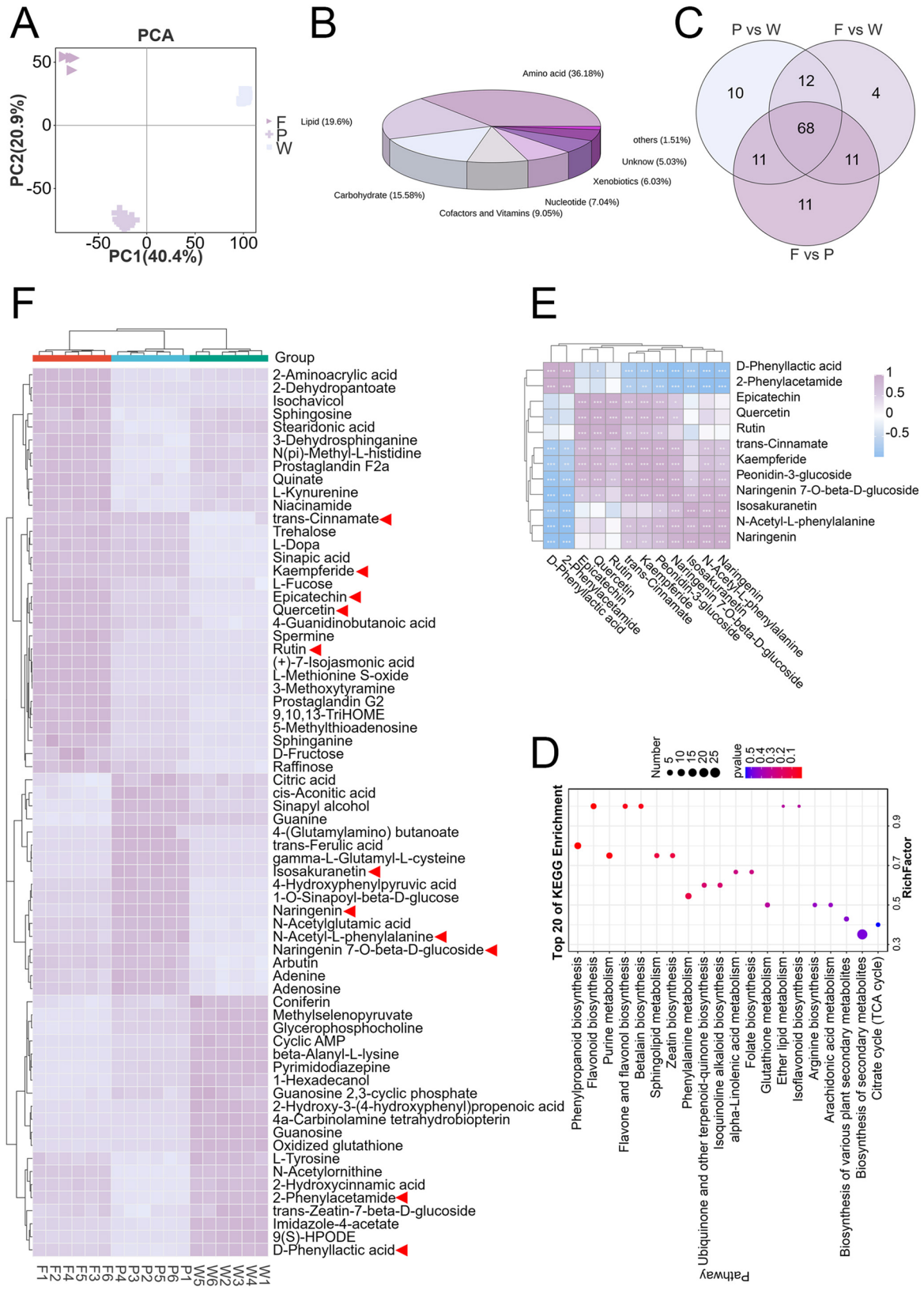

Fig. 3 Analysis of DM among W, P and F. (**A**) PCA of all metabolites; (**B**) Classification map of 199 metabolites identified via LC-MS/MS; (**C**) Venn diagram showing the overlap of DM identified via LC-MS/MS in the three groups; (**D**) Scatter plot of the top 20 KEGG-enriched pathways for 68 DM; (**E**) Pearson correlation analysis between peonodin-3-glucoside and eleven flavonoid metabolites. (**F**) Cluster heatmap of the 68 DM. Red triangle denotes the eleven flavonoid metabolites

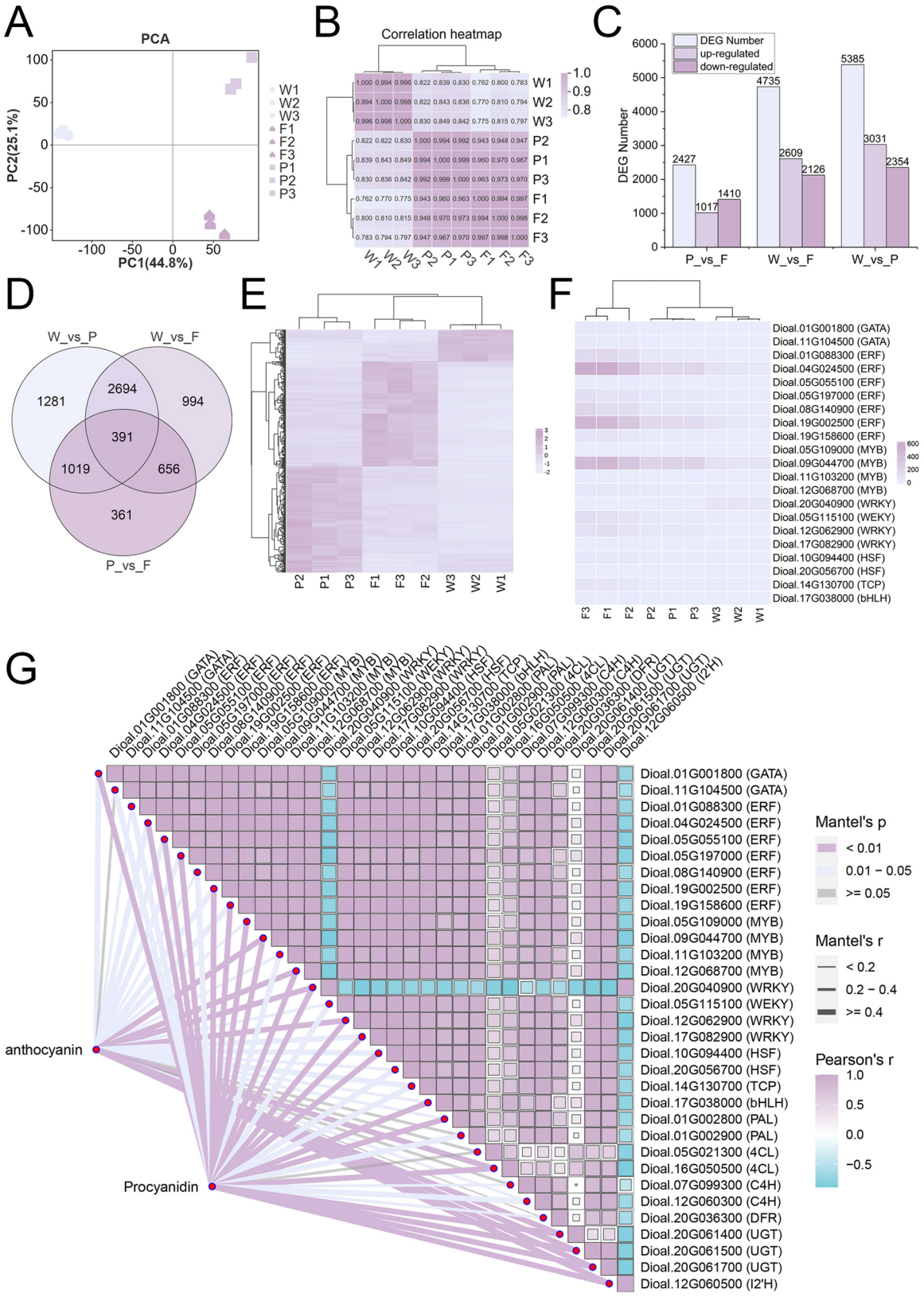

Fig. 4 (See legend on next page.)

(See figure on previous page.)

Fig. 4 Transcriptome analysis of W, P and F, as well as correlation analysis between core TFs, anthocyanins, procyanin and structural genes involved in anthocyanin biosynthesis. (**A**) PCA of all genes; (**B**) Pearson correlation analysis of the gene expression in each sample; (**C**) Number of DEGs in the three groups; (**D**) Venn diagram illustrates the overlap of DEGs among the three groups; (**E**) Cluster heatmap of 391 DEGs; (**F**) Identification of twenty-one TFs with consistent expression trends in the comparisons (P_vs_W, F_vs_W, F_vs_P); (**G**) Association analysis of twenty-one TFs, structural genes involved in anthocyanin biosynthesis and twenty-three differential anthocyanin metabolites

as *PAP1* and *PAP2*, which are involved in anthocyanin accumulation [22]. Under darkness conditions, MYB proteins are ubiquitinated by COP1 and subsequently degraded via the 26 S proteasome system, thereby influencing anthocyanin biosynthesis [31]. Under light conditions, the activity of *PpCOP1* is inhibited, leading to an increase in the levels of both *PpbHLH64* and *PpMYB10*. These TFs function downstream of *PpBBX18*, and form complexes with WD40 promoting biosynthesis of anthocyanins [17]. Moreover, phosphorylated MYB proteins under light conditions lead to enhanced biosynthesis of anthocyanins [32]. When plants are exposed to light, the SUMO E3 ligase SIZ can stabilize *MYB75*, leading to increased anthocyanin levels [33]. Three partially redundant TFs, *MYB11*, *MYB12*, and *MYB111*, regulate the expression of early biosynthetic genes and the accumulation of flavonols in *Arabidopsis* seedlings [34]. The transcriptional regulation of anthocyanin biosynthetic genes involves an MBW complex composed of WD40 protein, such as Transparent Testa Glabra 1 (*TTG1*), MYB TFs (e.g., *MYB75*, *MYB90*, *MYB113* and *MYB114*) and bHLH TFs, including *TT8*, Glabra 3 (*GL3*), and Enhancer of Glabra 3 (*EGL3*) [35]. In the study, MYBs, ERFs, and WRKYs associated to anthocyanins and structural genes in anthocyanin biosynthesis pathway were identified as key TFs. Specially, *DoMYB44* associated with procyanidins and anthocyanins was strongly induced under light condition. These findings indicated that MYB TFs are core regulators of anthocyanin content under light conditions in yam.

Transcriptome analysis indicated significant differences in the expression levels of structural genes, such as *PAL*, *C4H*, *4CL*, *DFR*, *UFGT*, *UGT*, *I2'H*, *BZ1*, and *3MaT1*, which are involved in phenylpropanoid biosynthesis, flavonoid biosynthesis, flavone and flavonol biosynthesis, as well as anthocyanin biosynthesis. These differences were observed between two plant varieties and were influenced by light conditions. These results suggest that potential TFs coordinately regulate the expression levels of structural genes involved in the aforementioned biosynthetic pathways, thereby affecting the metabolites within these pathways. In this study, we identified four TFs: *DoMYB44*, *DoMYB77*, *DoWRKY51* and *DoWRKY33.* These TFs associated with anthocyanins and structural genes involved in anthocyanin biosynthesis. The expression patterns of these four TFs and the structural genes in anthocyanin biosynthesis were consistent and strongly induced by light, especially *DoMYB44* and *DoMYB77*. In other plants, *MYB44* plays a critical role in anthocyanin biosynthesis [36, 37]. These findings indicate that *DoMYB44* may be a strong candidate gene for regulating anthocyanin biosynthesis under light conditions. However, the function of candidate genes in regulating anthocyanin biosynthesis needs to be further verified via experiment.

Conclusions

We have elucidated the differences in metabolite and genes expression between white and purple yams, as well as investigated the impact of light on metabolites and genes expression. We have identified four candidate transcription factors that regulated anthocyanin synthesis in yams and was responsive to light. This study fills a gap in understanding TFs involved in the molecular regulation of anthocyanin biosynthesis in yams. In the follow-up research, we will verify the functions of candidate genes and clarify the molecular networks they regulate. Additionally, the elucidation of the impact of light on anthocyanin content can aid in increasing anthocyanin levels in yam root tubers by altering cultivation conditions.

Materials and methods

Plant materials and growth conditions

Two yam varietyies, 'Luhe' (White root tuber) and 'Xuwen' (Red root tuber) with differential color, from Guangdong Academy of Agricultural Sciences (Guangzhou, China) were disinfected with 0.3% carbendazim for 30 min and then planted in the field. High ridge cultivation was adopted, with a plant spacing of 40 cm and a row spacing of 80 cm, and about 50 kg of NPK compound fertilizer (15-15-15) was applied per 667 m^2. After planting for 5 months (about the root swelling period), remove the soil on the top of the root tubers of 'Xuwen' variety and expose the top of the root tubers to natural light. One month later, the normal growth of 'Luhe' (White root tuber, W) and 'Xuwen' (Part red root tuber, P), and the exposed to light 'Xuwen' (Full red root tubers, F) were collected for transcriptome and metabolomics analysis. Three biological replicates were collected to frozen in liquid nitrogen and stored at -80℃.

Extraction and determination of total anthocyanins

The yams, which had been peeled, were sliced into thin slices with a thickness of 1–3 mm. A complex color fixative consisting of 0.05% citric acid, 0.10% sodium chloride, and 0.35% sodium ascorbate was applied at room

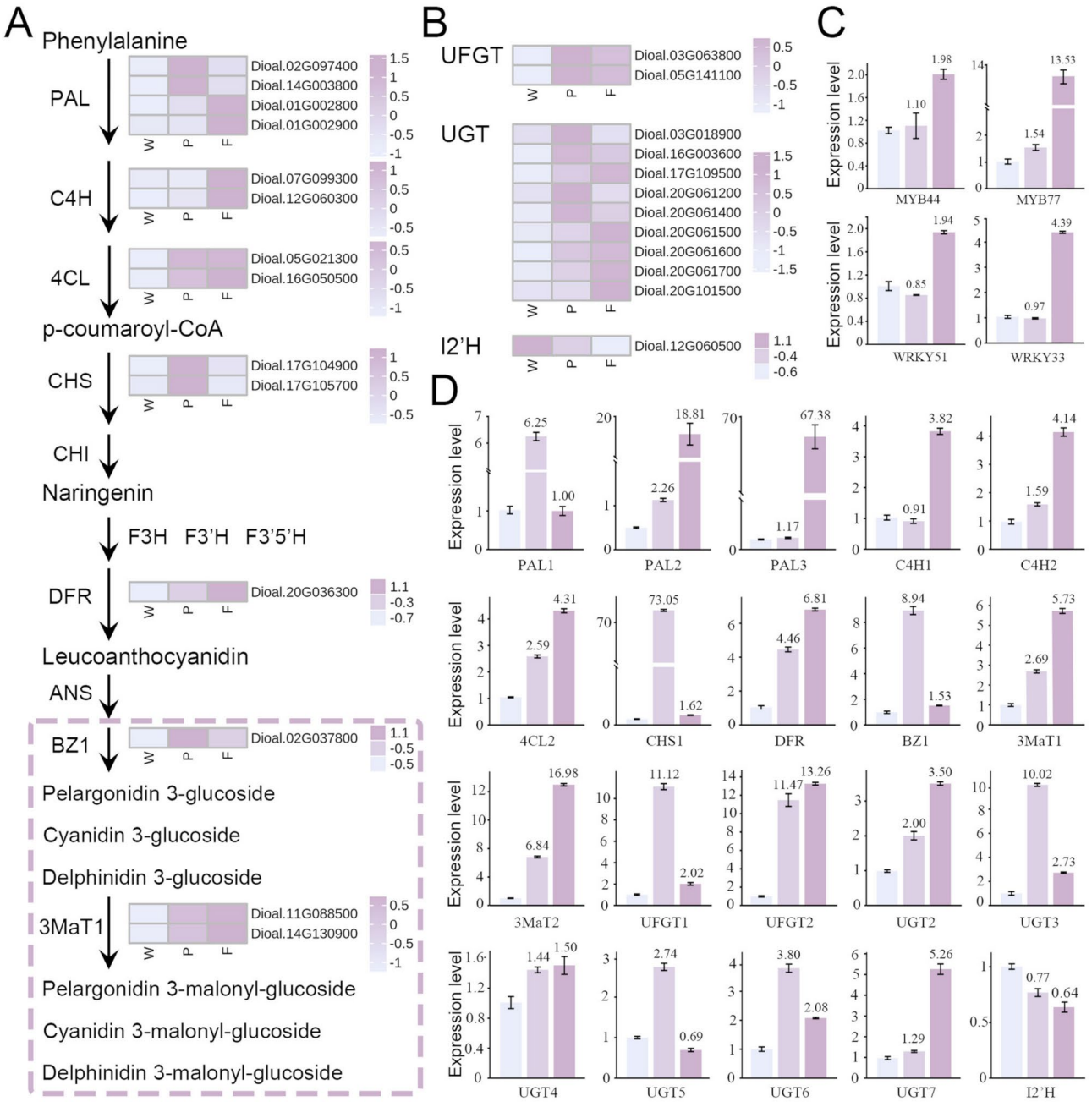

Fig. 5 Transcriptome and RT-qPCR analysis of core TFs and structural genes involved in anthocyanin biosynthesis. (**A**) Schematic diagram of anthocyanin biosynthesis and the expression levels of structural genes. Phenylalanine (PAL), cinnamic acid 4-hydroxylase (C4H), and 4-coumaric acid CoA ligase (4CL), chalcone synthase (CHS), chalcone isomerase (CHI), flavanone 3'-hydroxylase (F3H), flavonoid 3',5'-hydroxylase (F3'5'H), dihydroflavonol 4-reductase (DFR), anthocyanidin synthase (ANS), anthocyanidin 3-O-glucosyltransferase (BZ1), anthocyanin 3-O-glucoside-6"-O-malonyltransferase (3MaT1); (**B**) The expression levels of UFGTs and UGTs involved in phenylpropanoid biosynthesis, flavonoid biosynthesis, flavone and flavonol biosynthesis in 'Luhe' (W), 'Xuwen' (P) and and 'Xuwen-L' (F). UDP-glycose: flavonoid glycosyltransferase (UFGT), UDP-glycosyltransferase (UGT), isoflavone 2'-hydroxylase (I2'H); (**C**) RT-qPCR analysis of core TFs; (**D**) RT-qPCR analysis of structural genes involved in anthocyanin biosynthesis

temperature for 15 min. The citric acid, sodium ascorbate, and sodium chloride used were analytically pure reagents purchased from China National Pharmaceutical Group Chemical Reagent Co., Ltd. Distilled water was added at a ratio of 1:6 g/mL, and the mixture was homogenized using a tissue homogenizer. Anthocyanins were extracted using an ultrasonic extractor at a temperature of 30 °C, extraction time of 30 min, and ultrasonic power of 300 W. The homogenate was centrifuged at 4,000 rpm to separate the residue.

The determination of anthocyanin content was conducted using the dual-wavelength pH differential

method. A 1.00 mL aliquot of the sample solution was diluted to 10.00 mL with buffer solutions of pH 1.0 and 4.5, respectively. The pH 1.0 buffer solution was prepared by accurately weighing 1.49 g of potassium chloride and diluting it with distilled water to 100 mL. Then, 1.7 mL of hydrochloric acid was measured out and diluted with distilled water to 100 mL to create a 0.2 mol/L hydrochloric acid solution. The potassium chloride solution and hydrochloric acid solution were mixed in a 25:67 ratio and the pH was adjusted to 1.0 using the potassium chloride solution. For the pH 4.5 buffer solution, 1.64 g of sodium acetate was accurately weighed and diluted with distilled water to 100 mL, and the pH was adjusted to 4.5 using hydrochloric acid. The absorbance of the two solutions was measured at wavelengths of 700 nm and 540 nm. Each sample was determined in triplicate, and the average value was used to calculate the anthocyanin content according to the following formula: anthocyanin content (mg/100 g) = (A/ƐL)×MW×DF×V/Wt×100. In this formula, A represents the absorbance value, calculated as $A=(A_{540nm}-A_{700nm})_{PH1.0}-(A_{540nm}-A_{700nm})_{PH4.5}$. MW represents the relative molecular weight (449.2) of cyanidin-3-glucoside, and Ɛ represents the molar extinction coefficient of cyanidin-3-glucoside, which is 26,900 L/(mol·cm). Wt is the sample mass in grams, V is the final volume in milliliters after dilution, DF is the dilution factor, and L is the width (1 cm) of the cuvette.

Targeted Anthocyanidin metabolome assay

HPLC-grade methanol was purchased from Merck (Darmstadt, Germany), while MilliQ water (Millipore, Bradford, USA) was used in all experiments. Standard substances were purchased from isoReag (Shanghai, China), formic acid from Sigma-Aldrich (St Louis, MO, USA), and hydrochloric acid from Xinyang Chemical Reagent (China). Stock solutions of standards were prepared at a concentration of 1 mg/mL in 50% methanol and stored at -20 °C. They were then diluted with 50% methanol to working solutions prior to analysis. Samples were freeze-dried, ground into a powder by vibration grinder (JXFSTPRP-48, 30 Hz, 1.5 min), and stored at -80 °C. A 50 mg portion of the powder was weighed and extracted with 0.5 mL of methanol/water/hydrochloric acid (500:500:1, V/V/V). The extract was vortexed for 5 min, sonicated for 5 min, and centrifuged at 12,000 g under 4 °C for 3 min. The residue was re-extracted using the same procedure. The supernatants were collected, filtered through a membrane filter (0.22 μm, Anpel), and subjected to LC-MS/MS analysis.

Anthocyanidin content was detected using the AB Sciex QTRAP 6500 LC-MS/MS platform by MetWare (http://www.metware.cn/). The sample extracts were analyzed with a UPLC-ESI-MS/MS system (UPLC, ExionLC™ AD, MS Applied Biosystems 6500 Triple Quadrupole). The UPLC conditions were setted as follows: the column was Waters ACQUITY BEH C18 (1.7 μm, 2.1 mm*100 mm); the solvent system was water (0.1% formic acid): methanol (0.1% formic acid); the gradient program was 95:5 V/V at 0 min, 50:50 V/V at 6 min, 5:95 V/V at 12 min, held for 2 min, 95:5 V/V at 14 min, held for 2 min; the flow rate was 0.35 mL/min; the temperature was 40 °C; and the injection volume was 2 μL. Linear ion trap and triple quadrupole scans were acquired on a QTRAP® 6500 + LC-MS/MS System equipped with an ESI Turbo Ion-Spray interface, operating in positive ion mode and controlled by Analyst 1.6.3 software (Sciex). The ESI source operation parameters included: ion source - ESI+; source temperature – 550℃; ion spray voltage (IS) – 5500 V; curtain gas was set at 35 psi.

Anthocyanidins were analyzed using scheduled multiple reaction monitoring (MRM). Data acquisitions were performed using Analyst 1.6.3 software (Sciex). Quantification of all metabolites was conducted using Multiquant 3.0.3 software. The mass spectrometer parameters, including the optimized declustering potentials and collision energies for individual MRM transitions, were used. Specific MRM transitions were monitored for each elution period based on the metabolites of interest. Differentially expressed metabolites were identified based on a fold change ≥ 2 or fold change ≤ 0.5. The metabolites were annotated using the KEGG compound database (http://www.kegg.jp/kegg/compound/), and mapped to the KEGG database (http://www.kegg.jp/kegg/pathway.html). Pathways containing significantly expressed metabolites underwent metabolite set enrichment analysis using *p*-values from the hypergeometric test to determine their significance. Principal component analysis, correlation analysis, venn diagram, and cluster heat map were performed using online tools provided on their respective websites (https://cloud.metware.cn/#/tools/tool-list and https://www.omicshare.com/tools/). Three biological replicates were employed from the 'Luhe', 'Xuwen' and 'Xuwen-L'.

Non-targeted metabolome assay

Accurately weigh 200 mg (± 1%) of the sample into a 2 mL EP tube. Added 0.6 mL of methanol containing 2-chlorophenylalanine (4 ppm) at -20 ℃. Vortexed the mixture for 30 s. Then, added 100 mg of glass beads to the tube and placed it in a tissue grinding machine. Ground the samples at 50 Hz for 60 s. After grinding, sonicated the samples at room temperature for 15 min. Centrifuged the samples at 25 ℃ for 10 min at 12,000 rpm. Filtered the supernatant through a 0.22 μm membrane to obtain the prepared samples for LC-MS analysis. For quality control purposes, took 20 μL from each sample to monitor deviations in the analytical results. These QC samples

were compared to errors caused by the analytical instrument itself. The remaining samples were used for LC-MS detection.

Metabolite content was detected using Panomix (https://www.panomix.com/). Chromatographic sepa ration was achieved using a Thermo Vanquish system equipped with an ACQUITY UPLC® HSS T3 column (150 × 2.1 mm, 1.8 μm, Waters) maintained at 40 ℃. The autosampler temperature was set at 8 ℃. Gradient elution of analytes was carried out using 0.1% formic acid in water (B2) and 0.1% formic acid in acetonitrile (A2), or 5 mM ammonium formate in water (B1) and acetonitrile (A1) at a flow rate of 0.25 mL/min. Each sample was injected at 2 μL after equilibration. A linear gradient of solvent A (v/v) was applied as follows: 0 ~ 1 min, 2% A2/A1; 1 ~ 9 min, 2%~50% A2/A1; 9 ~ 12 min, 50%~98% A2/A1; 12 ~ 13.5 min, 98% A2/A1; 13.5 ~ 14 min, 98%~2% A2/A1; 14 ~ 20 min, 2% A2-positive model (14 ~ 17 min, 2% A1-negative model).

The ESI-MSn experiments were performed using the Thermo Q Exactive Focus mass spectrometer with a spray voltage of 3.8 kV and − 2.5 kV in positive and negative modes, respectively. The sheath gas and auxiliary gas were set at 30 and 10 arbitrary units, respectively. The capillary temperature was maintained at 325 ℃. The analyzer scanned a mass range of m/z 81 − 1,000 for full scan at a mass resolution of 70,000. Data-dependent acquisition MS/MS experiments were conducted with HCD scan at a normalized collision energy of 30 eV. Dynamic exclusion was implemented to remove unnecessary information in the MS/MS spectra.

Differentially expressed metabolites between two given samples were identified based on a one-way ANOVA p-value ≤ 0.05 and VIP ≥ 1. The identification of metabolites initially confirms the precise molecular weight of the metabolite (with a molecular weight error < 15 ppm). Subsequently, the metabolite is annotated with accurate information based on the fragment information obtained from the MS/MS mode in Metlin (http://metlin.scripps.edu), MoNA (https://mona.fiehnlab.ucdavis.edu//), and in-house standard compound databases at Panomix. Principal component analysis, correlation analysis, venn diagram, cluster heatmap, and scatter plot of KEGG enrichment were performed using online tools provided on their respective websites (https://cloud.metware.cn/#/tools/tool-list and https://www.omicshare.com/tools/). Six biological replicates were employed from the 'Luhe', 'Xuwen' and 'Xuwen-L'.

RNA-seq analysis

Total RNA was extracted and purified from root tubers by a MiniBEST Plant RNA Extraction Kit (TaKaRa, Dalian, China). The integrity and quality of the purified RNA were assessed by micro spectrophotometer and 1% agarose gel electrophoresis. Library construction, and sequencing were executed by Biomarker Technologies Co., Ltd (Beijing, China). To improve reliability, three biological replicates was used for Illumina deep RNA sequencing to decrease biological error. The reference genome data used for alignment was obtained from JGI (https://phytozome-next.jgi.doe. gov/info/Dalata_v2_1). The expression levels of each gene were quantified using the fragments per kilobase of transcript per million fragments mapped method. DEGs between two given samples were identified based on a fold change ≥ 2 and a false discovery rate (FDR) < 0.01. Principal component analysis, correlation analysis, venn diagram, cluster heatmap and association analysis were performed using online tools available on websites (https://cloud.metware.cn/#/tools/tool-list and https://www.omicshare.com/tools/).

RT-qPCR verified genes expression

RT-qPCR was employed to evaluate the expression levels of genes involved in flavonoid/anthocyanin biosynthesis. The primers used were listed in Table S13. Total RNA was extracted by a MiniBEST Plant RNA Extraction Kit (TaKaRa, Dalian, China). cDNA synthesis was performed using a HiScript II 1st strand cDNA synthesis Kit with gDNA eraser according to the manufacturer's instructions (Vazyme Biotech Co., Nanjing, China). All RT-qPCR reactions were conducted in Bio-Rad CFX96 with a 20 μl reaction volume using Taq Pro Universal SYBR qPCR Master Mix (Vazyme Biotech Co., Nanjing, China). Melting curves were generated to confirm the absence of nonspecific products in the reaction. The expression levels were normalized via the $2^{-\Delta\Delta CT}$ method, with the mRNA level of actin gene serving as the quantitative control. Three biological replicate samples were used for qRT-PCR analysis, and the reactions were performed in triplicate.

Abbreviations

PAL	Phenylalanine
C4H	Cinnamic acid 4-hydroxylasel
4CL	4-coumaric acid CoA ligase
CHS	Chalcone synthase
CHI	Chalcone isomerase
F3H	Flavanone 3′-hydroxylase
F3'5'H	Flavonoid 3′,5′-hydroxylase
DFR	Dihydroflavonol 4-reductase
BZ1	3-O-glucosyltransferase
3MaT1	Anthocyanin 3-O-glucoside-6″-O-malonyltransferase
MBW	MYB-bHLH-WD Repeat
PHY	PHYTOCHROME
CRY	CRYPTOCHROME
PCA	Principal component analysis
PC1	Principal component 1
PC2	Principal component 2
DEGs	Differentially expressed genes
DM	Differential metabolites

Supplementary Information

The online version contains supplementary material available at https://doi.org/10.1186/s12870-025-06738-w.

Supplementary Material 1

Supplementary Material 2

Author contributions

W.J.H and X.S.Q conceived and designed the paper. Z.P.P, Z.L, L.X.L, Q.J and L.W analyzed the experiments data. Z.P.P execute the manuscript. X.S.Q, W.J.H and C.S.K revised the manuscript. The final manuscript was approved by all authors.

Funding

The work was supported by the Work Funding Project for Rural Revitalization Local Branch and Expert Workstation of Guangdong Academy of Agricultural Sciences (2024 Workstation 05 and 07), General Survey and Collection of Agricultural Germplasm Resources in Guangdong Province in 2023 (0110), Zhejiang Provincial Natural Science Foundation (LY24C130003), Special Fund for Introducing Scientific and Technological Talents of Guangdong Academy of Agricultural Sciences (R2020YJ-YB3003).

Data availability

Sequence data that support the findings of this study have been deposited in the NCBI database under the accession number PRJNA1203071.

Declarations

Ethics approval and consent to participate

The experimental research on plants performed in this study complies with institutional, national and international guidelines.

Consent for publication

Not applicable.

Competing interests

The authors declare no competing interests.

Author details

[1]Guangdong Provincial Key Laboratory of Crops Genetics and Improvement, Crops Research Institute, Guangdong Academy of Agricultural Sciences, Guangzhou 510640, China
[2]Zhejiang Lab, Hangzhou 311100, China
[3]Yazhouwan National Laboratory, Sanya 572024, China
[4]Guangdong Provincial Engineering and Technology Research Center for Conservation and Utilization of the Genuine Southern Medicinal Resources, Guangzhou 510640, China

Received: 10 December 2024 / Accepted: 16 May 2025
Published online: 30 May 2025

References

1. Hu GJ, Zhao Y, Gao Q, Wang XW, Zhang JW, Peng X, Tanokura M, Xue YL. Functional properties of Chinese Yam (*Dioscorea opposita* thunb. Cv. Baiyu) soluble protein. J Food Sci Technol. 2018;55(1):381–8.
2. Li M, Chen LX, Chen SR, Deng Y, Zhao J, Wang Y, Li SP. Non-starch polysaccharide from Chinese Yam activated RAW 264.7 macrophages through the Toll-like receptor 4 (TLR4)-NF-κB signaling pathway. J Funct Foods. 2017;37:491–500.
3. Zhou Y, Farooqi AA, Xu B. Comprehensive review on signaling pathways of dietary saponins in cancer cells suppression. Crit Rev Food Sci Nutr. 2023;63(20):4325–50.
4. Eslami-Farsani M, Moslehi A, Hatami-Shahmir A. Allantoin improves histopathological evaluations in a rat model of gastritis. Physiol Int. 2018;105(4):325–34.
5. da Silva DM, Martins JLR, de Oliveira DR, Florentino IF, da Silva DPB, Dos Santos FCA, Costa EA. Effect of Allantoin on experimentally induced gastric ulcers: pathways of gastroprotection. Eur J Pharmacol. 2018;821:68–78.
6. Moriya C, Hosoya T, Agawa S, Sugiyama Y, Kozone I, Shin-Ya K, Terahara N, Kumazawa S. New acylated anthocyanins from purple Yam and their antioxidant activity. Biosci Biotechnol Biochem. 2015;79(9):1484–92.
7. Zheng XT, Yu ZC, Tang JW, Cai ML, Chen YL, Yang CW, Chow WS, Peng CL. The major photoprotective role of anthocyanins in leaves of *Arabidopsis thaliana* under long-term high light treatment: antioxidant or light attenuator? Photosynth Res. 2021;149:25–40.
8. Naing AH, Kim CK. Abiotic stress-induced anthocyanins in plants: their role in tolerance to abiotic stresses. Physiol Plant. 2021;172(3):1711–23.
9. Chen T, Hu S, Zhang H, Guan Q, Yang Y, Wang X. Anti-inflammatory effects of *Dioscorea alata* L. anthocyanins in a TNBS-induced colitis model. Food Funct. 2017;8(2):659–69.
10. Pomilio AB, Szewczuk NA, Duchowicz PR. Dietary anthocyanins balance immune signs in osteoarthritis and obesity–update of human in vitro studies and clinical trials. Crit Rev Food Sci Nutr. 2024;64(9):2634–72.
11. Shi MZ, Xie DY. Biosynthesis and metabolic engineering of anthocyanins in *Arabidopsis thaliana*. Recent Patents Biotechnol. 2014;8(1):47–60.
12. Wang J, Zhao Y, Sun B, Yang Y, Wang S, Feng Z, Li J. The structure of anthocyanins and the copigmentation by common micromolecular Copigments: A review. Food Res Int. 2024;176:113837.
13. Luan Y, Tang Y, Wang X, Xu C, Tao J, Zhao D. Tree peony R2R3-MYB transcription factor *PsMYB30* promotes petal blotch formation by activating the transcription of the anthocyanin synthase gene. Plant Cell Physiol. 2022;63(8):1101–16.
14. Gonzalez A, Zhao M, Leavitt JM, Lloyd AM. Regulation of the anthocyanin biosynthetic pathway by the TTG1/bHLH/Myb transcriptional complex in *Arabidopsis* seedlings. Plant J. 2008;53(5):814–27.
15. Wang XC, Wu J, Guan ML, Zhao CH, Geng P, Zhao Q. Arabidopsis MYB4 plays dual roles in flavonoid biosynthesis. Plant J. 2020;101(3):637–52.
16. Martinsen BK, Aaby K, Skrede G. Effect of temperature on stability of anthocyanins, ascorbic acid and color in strawberry and raspberry jams. Food Chem. 2020;316:126297.
17. Tao R, Yu W, Gao Y, Ni J, Yin L, Zhang X, Li H, Wang D, Bai S, Teng Y. Light-induced basic/helix-loop-helix64 enhances anthocyanin biosynthesis and undergoes CONSTITUTIVELY PHOTOMORPHOGENIC1-mediated degradation in Pear. Plant Physiol. 2020;184(4):1684–701.
18. Zhang YC, Gong SF, Li QH, Sang Y, Yang HQ. Functional and signaling mechanism analysis of rice CRYPTOCHROME 1. Plant J. 2006;46(6):971–83.
19. Li T, Yamane H, Tao R. Preharvest long-term exposure to UV-B radiation promotes fruit ripening and modifies stage-specific anthocyanin metabolism in highbush blueberry. Hortic Res. 2021;8(1):67.
20. Loyola R, Herrera D, Mas A, Wong DCJ, Höll J, Cavallini E, Amato A, Azuma A, Ziegler T, Aquea F. The photomorphogenic factors UV-B RECEPTOR 1, ELONGATED HYPOCOTYL 5, and HY5 HOMOLOGUE are part of the UV-B signalling pathway in grapevine and mediate flavonol accumulation in response to the environment. J Exp Bot. 2016;67(18):5429–45.
21. Wang Y, Zhang X, Zhao Y, Yang J, He Y, Li G, Ma W, Huang X, Su J. Transcription factor PyHY5 binds to the promoters of *PyWD40* and *PyMYB10* and regulates its expression in red Pear 'Yunhongli 1'. Plant Physiol Biochem. 2020;154:665–74.
22. Maier A, Schrader A, Kokkelink L, Falke C, Welter B, Iniesto E, Rubio V, Uhrig JF, Hülskamp M, Hoecker U. Light and the E3 ubiquitin ligase COP 1/SPA control the protein stability of the MYB transcription factors PAP 1 and PAP 2 involved in anthocyanin accumulation in *Arabidopsis*. Plant J. 2013;74(4):638–51.
23. Mattioli R, Francioso A, Mosca L, Silva P. Anthocyanins: A comprehensive review of their chemical properties and health effects on cardiovascular and neurodegenerative diseases. Molecules. 2020;25(17):3809.
24. Zhao Y, Jiang C, Lu J, Sun Y, Cui Y. Research progress of proanthocyanidins and anthocyanidins. Phytother Res. 2023;37(6):2552–77.
25. Zhou LJ, Wang Y, Wang Y, Song A, Jiang J, Chen S, Ding B, Guan Z, Chen F. Transcription factor *CmbHLH16* regulates petal anthocyanin homeostasis under different lights in *Chrysanthemum*. Plant Physiol. 2022;190(2):1134–52.
26. Guo X, Shakeel M, Wang D, Qu C, Yang S, Ahmad S, Song Z. Metabolome and transcriptome profiling unveil the mechanisms of light-induced anthocyanin synthesis in Rabbiteye blueberry (vaccinium Ashei: Reade). BMC Plant Biol. 2022;22(1):223.
27. Zeng H, Zheng T, Peng X, Tang Q, Xu H, Chen M. Transcriptomic and targeted metabolomics analysis of detached *Lycium ruthenicum* leaves reveals

mechanisms of anthocyanin biosynthesis induction through light quality and sucrose treatments. Metabolites. 2023;13(9):1004.
28. Ding R, Che X, Shen Z, Zhang Y. Metabolome and transcriptome profiling provide insights into green Apple Peel reveals light-and UV-B-responsive pathway in anthocyanins accumulation. BMC Plant Biol. 2021;21(1):351.
29. Zhang Y, Chen C, Cui Y, Du Q, Tang W, Yang W, Kou G, Tang W, Chen H, Gong R. Potential regulatory genes of light induced anthocyanin accumulation in sweet Cherry identified by combining transcriptome and metabolome analysis. Front Plant Sci. 2023;14:1238624.
30. Ma Y, Ma X, Gao X, Wu W, Zhou B. Light induced regulation pathway of anthocyanin biosynthesis in plants. Int J Mol Sci. 2021;22(20):11116.
31. Li YY, Mao K, Zhao C, Zhao XY, Zhang HL, Shu HR, Hao YJ. *MdCOP1* ubiquitin E3 ligases interact with MdMYB1 to regulate light-induced anthocyanin biosynthesis and red fruit coloration in Apple. Plant Physiol. 2012;160(2):1011–22.
32. Li S, Wang W, Gao J, Yin K, Wang R, Wang C, Petersen M, Mundy J, Qiu J-L. MYB75 phosphorylation by MPK4 is required for light-induced anthocyanin accumulation in *Arabidopsis*. Plant Cell. 2016;28(11):2866–83.
33. Zheng T, Li Y, Lei W, Qiao K, Liu B, Zhang D, Lin H. SUMO E3 ligase SIZ1 stabilizes MYB75 to regulate anthocyanin accumulation under high light conditions in Arabidopsis. Plant Sci. 2020;292:110355.
34. Stracke R, Ishihara H, Huep G, Barsch A, Mehrtens F, Niehaus K, Weisshaar B. Differential regulation of closely related R2R3-MYB transcription factors controls flavonol accumulation in different parts of the *Arabidopsis thaliana* seedling. Plant J. 2007;50(4):660–77.
35. Lloyd A, Brockman A, Aguirre L, Campbell A, Bean A, Cantero A, Gonzalez A. Advances in the MYB–bHLH–WD repeat (MBW) pigment regulatory model: addition of a WRKY factor and co-option of an anthocyanin MYB for betalain regulation. Plant Cell Physiol. 2017;58(9):1431–41.
36. Meng JX, Wei J, Chi RF, Qiao YH, Zhou J, Wang YL, Wang H, Li HH. MrMYB44-like negatively regulates anthocyanin biosynthesis and causes spring leaf color of Malus 'radiant'to fade from red to green. Front Plant Sci. 2022;13:822340.
37. Luan Y, Chen Z, Tang Y, Sun J, Meng J, Tao J, Zhao D. Tree peony PsMYB44 negatively regulates petal blotch distribution by inhibiting dihydroflavonol-4-reductase gene expression. Ann Botany. 2023;131(2):323–34.

Publisher's note